

INTERNATIONAL SOCIETY FOR SOIL MECHANICS AND GEOTECHNICAL ENGINEERING



This paper was downloaded from the Online Library of the International Society for Soil Mechanics and Geotechnical Engineering (ISSMGE). The library is available here:

<https://www.issmge.org/publications/online-library>

This is an open-access database that archives thousands of papers published under the Auspices of the ISSMGE and maintained by the Innovation and Development Committee of ISSMGE.

Plate anchor keying under inclined pullout in clay: observation and estimation

L'ancre de plaque keying dans le retrait incliné dans la glaise: observation et estimation

Z. Song

GHD Pty Ltd, Perth, Australia

Y. Hu

The University of Western Australia

ABSTRACT

The SEPLA (Suction Embedded Plate Anchor) is ideal for use in deep water oil and gas exploration. In this paper, transparent soil tests in centrifuge and numerical analysis using large deformation RITSS approach were conducted to study inlined pullout of plate anchors. The loss in anchor embedment during keying can be quantified by inspecting anchor movement in transparent soil or numerical study. This study is to correlate the actual anchor movement observed to that estimated using the chain displacement measured during anchor keying under inclined pullout.

RÉSUMÉ

Le SEPLA (Embedded Suction Anchor Plate) est idéal pour une utilisation en eau profonde exploration pétrolière et gazière. Dans ce document, la transparence des essais en centrifugeuse du sol et de l'analyse numérique utilisant de grandes déformations RITSS approche ont été menées pour étudier inlined retrait de la plaque d'ancrage. La perte d'ancrage dans l'incrustation au cours de la saisie peut être quantifiée par l'inspection d'ancrage dans le mouvement du sol ou de la transparence étude numérique. Cette étude est de corrélérer les ancrer le mouvement observé à celui estimé en utilisant la chaîne de déplacement mesurée au cours de la saisie en vertu d'ancrage incliné retrait.

Keywords : Anchor, Loss of embedment

1 INTRODUCTION

In recent years, oil and gas exploration has progressed into deep water areas to develop hydrocarbon fields. For water depths in excess of 500 m, conventional platforms are generally replaced by floating facilities, anchored to the seabed using catenary or taut-wire moorings. The latter type of mooring imparts significant vertical loading to the anchor, and consequently many different types of anchoring systems have been developed (Ehlers et al. 2004). The SEPLA (Suction Embedded Plate Anchor) is one such system where a suction caisson is used to embed a plate anchor that is slotted vertically into its base. After installation, a mooring line attached to the plate anchor is tensioned, causing the plate anchor to rotate or 'key' to an orientation that is perpendicular or almost perpendicular to the pullout direction. The SEPLA installation and keying processes are illustrated schematically in Figure 1 (Dove et al. 1998, Aubeny et al. 2001).

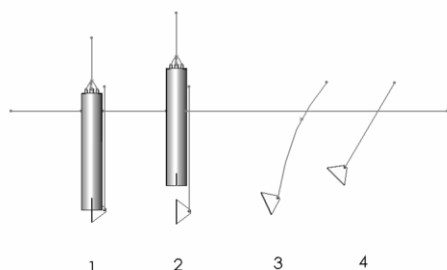


Figure 1 Installation and anchor keying processes for the Suction Embedded Plate Anchor (SEPLA)

The embedment depth will reduce as the plate rotates during pullout thus a non-recoverable loss in potential anchor capacity.

Reports on the loss of embedment of vertically installed anchors during keying show a large range. US Naval Civil Engineering Laboratory guidelines (NCEL, 1985) propose that the loss of embedment during anchor keying is twice the anchor breadth ($2B$) in cohesive soils, whilst recognising that the loss of embedment is also a function of anchor geometry, soil type, soil sensitivity and duration of time between penetration and keying. However, the anchor padeye eccentricity was not reported. More recently Wilde et al. (2001) reported in situ full scale and reduced scale onshore and offshore test results for SEPLAs in clay. Soil sensitivity was in the range 1.8 – 4.0 for the different test sites and the loss of embedment during keying was 0.5 to 1.7 times the anchor breadth B , with lower embedment losses corresponding to higher soil sensitivities.

In order to study the effect of loading eccentricity on the keying process, O'Loughlin et al. (2006) conducted strip anchor tests adjacent to a Perspex window in custom fabricated plane strain chambers located within a drum centrifuge channel. Plate anchor displacement was quantified through a series of digitally captured images of the clay-Perspex interface. Their results showed a strong dependence of loss in embedment on loading eccentricity (e).

The influence of suction installation on anchor keying and anchor capacity was investigated through a series of beam centrifuge tests in kaolin clay (Gaudin et al., 2006). They found that, for the keying of square anchors with $e/B = 0.66$ with 45° pullout, the loss in embedment after a jacked-in installation was in the range 1.3 to 1.5 B . The loss in anchor embedment was reduced to 0.9 to 1.3 B after suction installation. A strong correlation between the loading angle and the loss in anchor embedment was observed.

Large deformation finite element analyses and centrifuge model tests of plate anchor keying in clay were performed (Song and Hu 2008). The effects of anchor thickness, anchor padeye eccentricity, anchor submerged weight and soil disturbance were studied with anchors in uniform or normally

consolidated clays. Design equation are expressed to calculate the loss of embedment during keying for vertical and inclined pullout plate anchors in clay.

As outlined above, the current field and laboratory experimental results show a wide range of loss in anchor embedment during keying. Due to the obscurity of natural soils, the measurement on loss of vertical embedment can only be estimated using the back-analysis of anchor chain load-displacement data. In this paper, in order to provide more accurate estimation of anchor keying using anchor chain displacement data, transparent ‘soil’ tests in centrifuge and large deformation FE analyses are conducted to investigate the anchor keying process. Thus the actual anchor movement observed can be correlated to the chain displacement measured during anchor keying.

2 NUMERICAL METHODS

2.1 Large deformation FE analysis

Numerical analyses were conducted using the finite element (FE) package AFENA (Carter and Balaam 1990), with modifications to simulate the large deformations of soils. The RITSS (Remeshing and Interpolation Technique with Small Strain - Hu and Randolph, 1998a) approach has been chosen to simulate the continuous pullout of the anchor. As the name implies, a series of small-strain analysis increments are followed by frequent remeshing and interpolation of the field quantities (stresses and material properties) from the Gauss points in the old mesh to those in the new mesh.

To reduce computational time and to simplify the problem, a two dimensional strip plate anchor installed vertically in clay was analysed. The interface between the soil and the anchor plate was assumed to be rough. Since the plate anchor is normally installed deeply in soil, soil flow during anchor keying should be localised around the plate. Thus it is imposed that there is no detachment between the plate from the soil.

2.2 Anchor loading system

The plate anchor in the FE analyses comprises an anchor plate connected perpendicularly to a triangular anchor shank (see Figure 2). The anchor shank effect was studied by conducting analyses with and without shank weight (W_{shank}) and shank resistance (f). The loading eccentricity (e) is measured from the anchor padeye to the centreline of the anchor plate. The pullout force (F), for any loading direction, is initially applied vertically to the anchor padeye ($\theta_a = 90^\circ$). Upon anchor rotation, the loading angle at the padeye decreases, till the chain becomes straight and is perpendicular to the plate with $\theta_a = \theta_0$. This process can also be seen in Figure 1. During anchor rotation, the applied force at the anchor padeye results in an equivalent loading system including a horizontal force (F_H), a vertical force (F_V) and a moment (M) about the anchor centre. This loading system can be expressed as:

$$F_H = F \times \cos \theta_a + f \cos \beta \quad (1)$$

$$F_V = \begin{cases} F \times \sin \theta_a - W'_a - f \sin \beta & \text{for } F_V > 0 \\ 0 & \text{for } F_V < 0 \end{cases} \quad (2)$$

$$M = \begin{cases} F \times e \times \sin[\theta_a - (90 - \beta)] - f \times e_f - W'_a \times e_w \times \sin \beta & \text{for } M > 0 \\ 0 & \text{for } M < 0 \end{cases} \quad (3)$$

where θ_a is the angle of force F at the padeye to the horizontal (for vertical pullout, $\theta_a = 90^\circ$), θ is the initial pullout angle from pulley to anchor padeye, θ_0 is the chain angle (to the horizontal)

at the soil surface and β is the plate anchor inclination to the horizontal. The overall submerged anchor weight, W'_a , is the difference between the anchor weight in air and the anchor buoyancy force in soil. The buoyancy force of the anchor in soil was calculated as the anchor volume multiplied by the bulk unit weight of soil, which is $\gamma_s = 17 \text{ kN/m}^3$. The anchor weight in air was calculated using the steel unit weight of $\gamma_a = 77 \text{ kN/m}^3$. The eccentricity of W'_a is generated by the shank weight. The shank resistance f acts in the opposite direction of the anchor movement. During rotation, it was approximated as parallel to the anchor plate and located with an eccentricity e_f from the front face of the anchor.

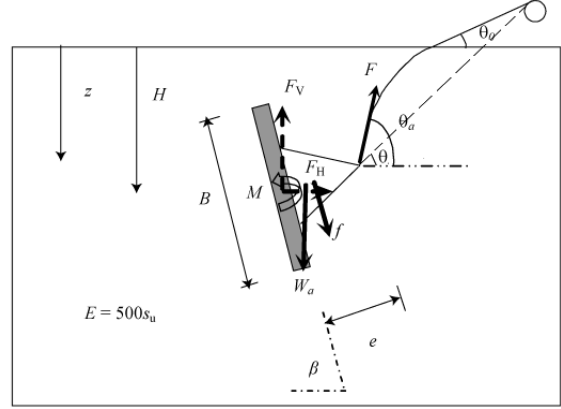


Figure 2 Setup of anchor in numerical analysis

2.3 Anchor chain analysis

For inclined anchor pull out, it is necessary to simulate the chain profile to account for the forces developed along the anchor chain. During inclined pullout, the anchor chain starts to slide and cut through the soil immediately after the pullout force is applied, and forms an inverted catenary profile. This profile can generate a significant frictional capacity along the length of the chain (Neubecker and Randolph 1995). The analytical solution proposed by Neubecker and Randolph (1995), which relates the chain orientation, the chain tension and the chain bearing resistance per unit length, was used in the present study to provide the chain profile at any given stage of anchor keying. Thus the chain tension force at the anchor padeye was calculated using:

$$\frac{F}{2} (\theta_a^2 - \theta_0^2) \approx \int_{z=0}^H Q dz = H \bar{Q} \quad (4)$$

where F is the chain tension at the padeye at depth H , Q is the chain bearing resistance at a depth z and \bar{Q} is the average bearing resistance (per unit length of chain) over the depth from soil surface ($z = 0$) to the padeye embedment depth H . The detailed chain profile formulas can be found in Neubecker and Randolph (1995).

Initially the anchor chain (and hence the force applied to the anchor) was assumed to be vertical at the padeye, i.e. $\theta_a = 90^\circ$. After the first step of remeshing in the FE analysis, the position of the anchor and the whole soil domain was updated according to the anchor and chain displacements. The new interaction point between the soil surface and chain system was then calculated and the updated θ_0 was used to calculate the new pullout angle θ_a from Eq. 4. This updating process was repeated throughout the keying process. The full procedure for the large deformation analysis of anchor keying may therefore be summarised as:

Step 1: Set up the initial force $F = 0$ at the padeye vertically ($\theta_a = 90^\circ$);

Step 2: Use Eqs 1-3 to calculate the equivalent forces and moment applied to the anchor;

Step 3: Conduct 50 small-strain incremental FE analyses with an incremental load control step of ΔF ;

- Step 4: Update anchor location and chain profile;
 Step 5: Calculate new θ_a using Eq. 4;
 Step 6: Apply the new force F with the new θ_a ;
 Step 7: Stop if the anchor ultimate bearing capacity has been reached; otherwise go to Step 2.

3 EXPERIMENTAL SETUP

The centrifuge tests were carried out using the UWA (University of Western Australia) drum centrifuge (Stewart et al. 1998), which has a diameter of 1.2 m with a channel of radial depth 0.2 m and height 0.3 m. The maximum rotational speed of the channel is 850 rpm, which is equivalent to a maximum acceleration of 485 g at the base of the channel, reducing to 364 g at the top of a 150 mm deep sample.

In order to observe the anchor rotational behaviour in soil during keying, physical tests were carried out in a pre-consolidated uniform transparent material in the drum centrifuge. This transparent material, which was made from 6 % by weight of fumed silica, (a mix, by volume, of 70 % paraffin and 30 % white spirit), has clay-sized particles and exhibits similar geotechnical properties to natural clay. The term 'transparent soil' has been used to refer to this material throughout the remainder of the paper. The detailed procedure for producing the transparent soil was reported by Gill (1999). The testing chamber is modular, allowing either side of each chamber to be replaced with a Perspex panel to facilitate observations of the test.

The reduced scale (1:100) model anchor was fabricated from 2 mm thick stainless steel to form a square plate anchor with model breadth = width = 40 mm, which is equivalent to a 4 m square anchor in prototype scale (i.e. under 100 g centrifuge acceleration). The eccentricity of the anchor padeye from the front face of the anchor plate was 25 mm (2.5 m in prototype scale). This corresponds to an eccentricity ratio of $e/B = 0.625$.

To facilitate optical measurement of the plate anchor keying process, a digital camera was placed within a custom made cradle, which supports the camera lens at high acceleration levels. The cradle was mounted securely in the drum channel and oriented such that the camera lens axis was perpendicular to the measurement plane. The testing arrangement in the drum centrifuge channel was set up according to the arrangement reported by White et al. (2003). A Canon S50 camera with a 5 Mega Pixel resolution (2592×1944 pixels) was used for digital image capture. The camera was set to continuous shooting mode, which, for the Canon S50, results in a full-resolution capture frequency of 0.5 Hz. Remote triggering of the camera was achieved using a small mass fixed to the shutter, which activated the camera into continuous shooting mode whenever the centrifuge acceleration was above a certain level (typically 25 g).

The anchor was installed manually at 1 g to a depth of 120 mm ($= 3B$) measured at the anchor centre. After installation, the strong box with soil sample was placed in the drum centrifuge channel and the centrifuge acceleration level was increased to achieve 100 g at the centre of the testing sample. Soil characterisation tests were performed using a T-bar penetrometer (Stewart & Randolph, 1994), from which a continuous profile of the undrained shear strength, s_u , was derived using the commonly adopted T-bar factor, $N_{Tbar} = 10.5$. A typical undrained shear strength profile of 18 kPa is observed. The anchor was pulled out with an inclined pullout angle of $\theta = 60^\circ$. The anchor chain was pulled out at a constant rate of $v = 0.25$ mm/s, which gives a dimensionless velocity of vB/c_v in excess of 30, ensuring soil undrained behaviour (Finnie and Randolph 1994).

4 RESULTS AND DISCUSSION

The effect of anchor pullout inclination on anchor keying has been studied using a centrifuge test in transparent soil and large deformation FE analysis.

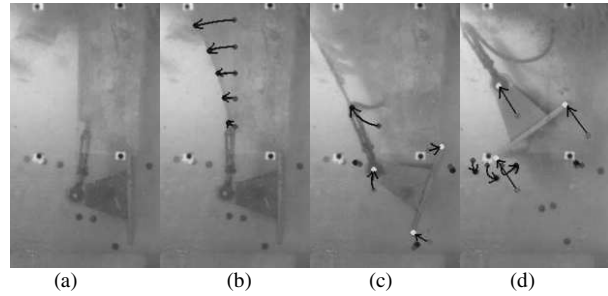


Figure 3 Transparent soil test

Four digital images from the transparent soil test are selected and displayed in Figure 3. From Figure 3a to Figure 3b, it is seen that the anchor chain cuts through the soil before the anchor starts to rotate. From Figure 3b, the anchor rotates half way by Figure 3c and reaches full rotation by Figure 3d. Figure 3d also shows the anchor translating through the soil after having completed its rotation, with the soil flowing around the anchor edges.

The relationship of the loss in anchor embedment during keying and anchor chain displacement is shown in Figure 4. The transparent soil test data and FE results of anchor keying are compared, and the good agreement between the test data and FE analysis result is apparent for anchor with shank. However, the shank effect is mainly on anchor rotating process, and is not significant on total loss in anchor embedment. Anchor position and pullout capacity are depicted in Figures 5 and 6 respectively. As can be seen in these figures, after anchor full rotation, the anchor centre has moved vertically upwards by $0.3 B$. Soil heave can be observed at the surface of the soil domain (Figure 5). The good agreement between the experimental and numerical trajectories in Figure 3 suggests that the numerical approach is robust to provide design information when anchor is simulated appropriately. Thus, it can be used as a practical tool when anchor geometry varies. It is also observed in Figure 6 that the anchor pullout capacity increase gradually from point 2 to point 3 and then dramatically from point 3 to point 4 to ultimate pullout capacity. This is a typical pullout response curve observed in Gaudin et al. (2006).

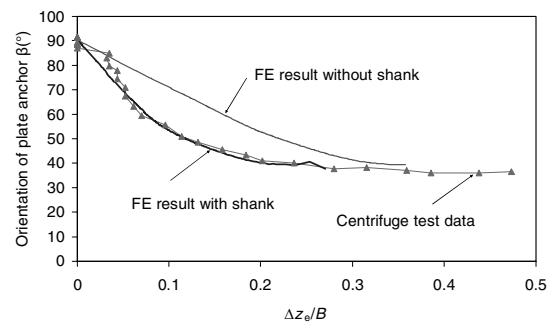


Figure 4 Comparison between FE results and transparent soil test data

To simplify the numerical simulation, the loss of embedment for plate anchor without shanks in clay is estimated by assuming that the anchor moves straight forward with a steady inclined angle of a 22.5° from point 2 to point 3 and a steady inclined angle of a 45° from point 3 to point 4. The measured and estimated results are shown in Figure 7. As can be seen from this figure, the estimated data of loss in anchor embedment agree well with measured FE results. Therefore, a pullout response curve can be used to estimate the loss in anchor embedment during keying.

Table 1 summarized estimation results for loss of anchor embedment data from published papers. As can be seen from this table, estimation by using the method from this paper

agrees well with the published data except Christophe (2006). This might be due to the loss in anchor embedment from Christophe (2006) is back-calculated, not observed.

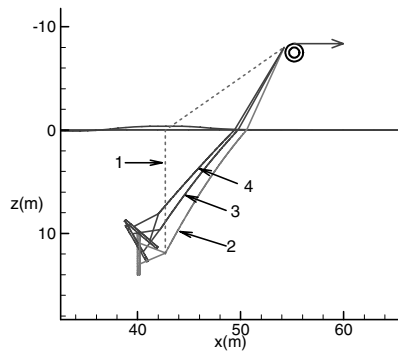


Figure 5 Anchor and chain position during pullout in FE analysis

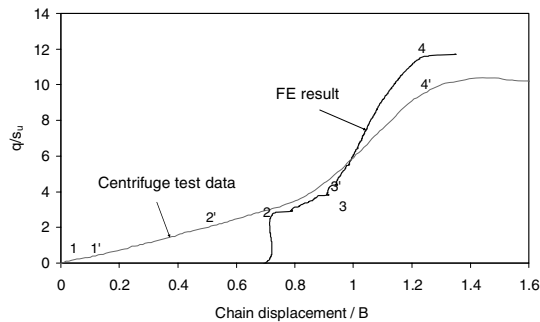


Figure 6 Pullout responses in FE analysis and transparent soil

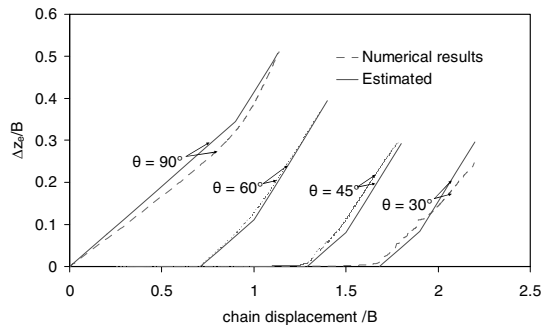


Figure 7 Loss of anchor embedment correlating to chain displacement

Table 1 Estimated loss of embedment

	Reported (with shank)	Estimated (no shank)
Song and Hu (2007) 60°	0.27	0.38
Christophe et al. (2006) 45°	~1.33 (estimation)	~0.46

5 CONCLUSIONS

In this paper, transparent ‘soil’ tests in centrifuge and large deformation FE analyses were conducted to investigate the anchor keying process. Anchor rotation and loss in anchor embedment during keying were observed in transparent soil test and large deformation FE analysis. It is found that the large deformation FE analysis can provide accurate positioning of anchor during keying. Both test data and FE result show that, during inclined anchor pullout, the anchor experienced chain cutting soil, initial rotation to half-way, full rotation and anchor capacity development. The correlation between the loss in anchor embedment and the chain displacement was proposed. This correlation showed working well with the FE results and

centrifuge test data from observation. Thus it can be used in offshore practice when only the response of chain displacement and anchor capacity during keying is available.

ACKNOWLEDGEMENT

The research presented here is supported by the Australian Research Council (ARC) through the Discovery Project scheme (DP0344019). This support is gratefully acknowledged. Experiments could not have been performed without the support of the Centre for Offshore Foundation Systems (COFS).

REFERENCE:

Aubeny, C. P., Murff, D. J., and Roesset, J. M. 2001. Geotechnical issues in deep and ultra deep waters. *International Journal of Geomechanics*, 1(2), 225 - 247.

Carter, J. P. and Balaam, N. 1990. AFENA Users Manual, Geotechnical Research Centre, The University of Sydney.

Dove, P., Treu, H., and Wilde, B. 1998. Suction embedded plate anchor (SEPLA): a new anchoring solution for ultra-deepwater mooring. *Proc. Deep Offshore Tech. Conf.*, New Orleans, USA.

Ehlers, C. J., Young, A. G. and Chen J. H. 2004. Technology assessment of deepwater anchors. *Proceedings of Annual Offshore Technology Conference*, Houston, Texas, U.S.A., 3-6 May 2004, OTC 016840.

Finnie, I. M. S., and Randolph, M. F. 1994. Punch-through and liquefaction induced failure of shallow foundations on calcareous sediments. *Proc. Int. Conf. on Behaviour of Offshore Structures*, Boston, USA., 217-230.

Gaudin, C., O’Loughlin C. D., Randolph, M. F. and Lowmass, A. C. 2006. Influence of the installation process on the performance of suction embedded plate anchors. *Géotechnique* 56(6): 381-391.

Gill, D. R. 1999. Experimental and theoretical investigations of pile and penetrometer installation in clay, PhD. Thesis, Trinity College, Dublin.

Hu, Y., and Randolph, M. F. 1998a. H-adaptive FE analysis of elastoplastic non-homogeneous soil with large deformation. *Computers and Geotechnics*, 23(1-2), 61-83.

Hu, Y., and Randolph, M. F. 1998b. A practical numerical approach for large deformation problems of soil. *International Journal for Numerical and Analytical Methods in Geomechanics*, 22(5), 327-350.

NCEL, 1985. *Handbook for Marine Geotechnical Engineering*, US Naval Civil Engineering Laboratory, Port Hueneme, California, USA.

Neubecker, S. R., and Randolph, M. F. 1995. Profile and frictional capacity of embedded anchor chains. *Journal of Geotechnical Engineering*, 121(11), 797-803.

O’Loughlin, C. D., Lowmass, A., Gaudin, C., and Randolph, M. F. 2006. Physical modelling to assess keying characteristics of plate anchors. *International Conference on Physical Modelling in Geotechnics 2006*, Hong Kong.

Randolph, M. F., Cassidy, M. J., Gourvenec, S., and Erbrich, C. 2005. Challenges of Offshore Geotechnical Engineering. *Proc. 16th Int. Conf. on Soil Mech. and Geotech. Engrg*, Osaka, Japan, 1:123-176.

Song, Z. and Hu, Y. 2008. Large Deformation FE Analysis of Plate Anchor Keying in Clay. *The 12th International Conference of International Association for Computer Methods and Advances in Geomechanics (IACMAG)*, Goa, India

Song, Z. and Hu, Y. 2008. Suction embedded plate anchor test in centrifuge. *Proceedings of 10th Australia New Zealand Conference on Geomechanics*, Brisbane, Australia, pp. 562-567.

Stewart, D. P., Boyle, R. S., and Randolph, M. F. 1998. Experience with a new drum centrifuge. *Proc. Int. Conf. Centrifuge '98*, Tokyo, Japan, 35-40.

Stewart, D. P., and Randolph, M. F. 1994. T-bar penetration testing in soft clay. *J Geotech. Engr. Div.*, ASCE, 120(12), 2230-2235.

White, D. J., Take, W. A., and Bolton, M. D. 2003. Soil deformation measurement using particle image velocimetry (PIV) and photogrammetry. *Géotechnique*, 53(7), 619-631.

Wilde, B., Treu, H., and Fulton, T. 2001. Field testing of suction embedded plate anchors. *11th (2001) International Offshore and Polar Engineering Conference*, Jun 17-22 2001, Stavanger, 544-551.